Voltammetry and Growth Physiology of *Geobacter sulfurreducens* Biofilms as a Function of Growth Stage and Imposed Electrode Potential

Enrico Marsili,[a] *Jian Sun*,[b] *Daniel R. Bond*[a,c]*

[a] BioTechnology Institute, University of Minnesota, St. Paul, Minnesota 55108, USA
[b] Department of Environmental Science and Engineering, South China University of Technology, Guangzhou 510006, P. R. China
[c] Department of Microbiology, University of Minnesota, Minneapolis, Minnesota 55455, USA
*e-mail: dbond@umn.edu

Received: June 15, 2008
Accepted: October 1, 2009

Abstract
The ability of *Geobacter sulfurreducens* to utilize electrodes as electron acceptors provides a system for monitoring mechanisms of electron transfer beyond the cell surface. This study examined the physiology of extracellular electron transfer during many stages of growth, and in response to short- and long-term changes in electron acceptor potential. When *G. sulfurreducens* was grown on planar potentiostat-controlled electrodes, the magnitude of early cell attachment increased with initial cell density. However, the first cells to attach did not demonstrate the same electron transfer rates as cells grown on electrodes. For example, following initial attachment of fumarate-grown cells, the electron transfer rate was 2 mA/mg protein, but increased to nearly 8 mA/mg protein within 6 h of growth. Once attached, all biofilms grew at a constant rate (doubling every 6 h), and sustained a high specific electron transfer rate and growth yield, while current density was below 300 $\mu A/cm^2$. Beyond this point, the rate of current increase slowed and approached a stable plateau. At all phases, slow scan rate cyclic voltammetry of *G. sulfurreducens* showed a similar well-defined sigmoidal catalytic wave, indicating the general model of electron transfer to the electrode was not changing. Short-term exposure to reducing potentials (3 h) did not alter these characteristics, but did cause accumulation of electrons which could be discharged at potentials above -0.1 V. Sustained growth at lower potentials (-0.16 V) only slightly altered the pattern of detectable redox species at the electrode, but did eliminate this pattern of discharge from the biofilm. Single-turnover voltammetry of colonized electrodes showed at least 3 redox couples at potentials similar to other recent observations, with redox protein coverage of the electrode on the order of ca. 1 $nmol/cm^2$. The consistent electrochemistry, growth rate, and growth yield of the *G. sulfurreducens* biofilm at all stages suggests an initial phase where cells must optimize attachment or electron transfer to a surface, and that after this point, the rate of electron production by cells (rate electrons are delivered to the external surface) remains rate limiting compared to the rate electrons can be transferred between cells, and to electrodes.

Keywords: *Geobacter*, Voltammetry, Biofilm, Fuel cells

DOI: 10.1002/elan.200800007

1. Introduction

Bacteria with an ability to utilize metals in anaerobic respiration (such as *Geobacter spp., Shewanella spp. Geothrix fermentans,* and *Rhodoferax ferrireducens*) possess a mechanism for generating ATP while transferring electrons beyond their outer surface [1–6]. The consequences of this electron transfer have been extensively studied in the context of Fe and Mn biogeochemistry [7, 8], hydrocarbon and U(VI) bioremediation [9–11], and microbially influenced corrosion [12, 13]. More recently, some metal-reducing bacteria have been shown to use electrodes as terminal electron acceptors, and such electrode-reducing bacteria have been termed 'electrochemically active' [14], 'electricigens' [15, 16], 'exoelectrogenic' [17], and 'anodophillic' [18].

While there are many general demonstrations of bacterial growth with electrodes as the terminal electron acceptor, the mechanisms controlling electron flow from the microbial cell interior to metals or electrodes are not well understood. This is partially due to complexity; multiple redox proteins must cooperate to transfer electrons from the cytoplasm to the outer cell surface (a distance of 50–100 Å) , and then outer surface proteins must be brought within 5–10 Å of a metal oxide or electrode for efficient electron transfer to take place. As electrons flow out of the cell, their rate of transfer could be impeded by internal redox status, (NAD:NADH ratios), feedback from proton motive force generation, diffusion rates within the periplasm, availability of redox shuttles secreted by the organism, and protein:surface kinetics [19–21].

This complexity can also be seen in results from genetic analyses. For example, in *Geobacter*, insertions in genes for periplasmic cytochromes (such as PpcA), membrane cytochromes (including MacA, OmcB, OmcC, OmcE, OmcF,

OmcS, OmcT, OmcZ), other outer membrane proteins (OmpB, OmpJ), and subunits of type IV pili with conductive properties (PilA) [22–24], have all resulted in defects in electron transfer to extracellular acceptors [25–30]. However, disruption of some cytochromes (OmcF or or MacA) [31], outer membrane proteins (OmpJ) [31, 32] secretion machinery subunits (OxpG) [30], and even type IV pili subunits [33] has also been shown to alter localization of key cytochromes to the *Geobacter* membrane, or lead to compensating adaptive mutations, complicating interpretation of mutant data. This list suggests that electron transfer beyond the *Geobacter* surface could proceed via an array of pathways, each tuned to different redox conditions or growth stages. Alternatively, this data could suggest a redundant collection of redox proteins, analogous to the mixture of enzymes used by cellulose-degrading bacteria, that allows *Geobacter* to successfully interact with the diversity of iron oxide surfaces present in the environment.

Methods for cultivating cells on defined electrodes have recently shown that voltammetry can measure extracellular electron transfer from viable biofilms of *Geobacter* [26, 34, 35] and *Shewanella spp.* [26] to the electrode. Key findings from these early studies include the fact *G. sulfurreducens* biofilms grown to maturity (10–20 μm thick) respond with remarkably simple kinetics, especially considering the perceived complexity of the number of steps required to deliver electrons such long distances. These studies demonstrated the ability of voltammetry and electrochemical impedance spectroscopy techniques to determine midpoint potentials and voltage-dependent rates in intact electron transport chains.

In this report, we investigated *G. sulfurreducens* biofilms at different stages of growth, providing evidence that electron transfer to an external electrode (and growth of new cells) proceeds at rates typically observed for planktonic *G. sulfurreducens* cells utilizing soluble Fe(III). In all experiments, electron transfer was via a pathway that responded similarly to adjustment of driving force across a defined potential range. Voltammetry at different stages of colonization was consistent with the general mechanism of extracellular electron transfer remaining the same, and growth at lower potentials did not significantly alter the electron transfer process. In addition, cyclic voltammetry of attached biofilms under nonturnover conditions confirmed the presence multiple redox species adsorbed to the electrode. This quantitative data provides a more complete picture of extracellular respiration during multiple phases of biofilm growth, and points to mechanisms that could enable more efficient extracellular electron transfer to metals and electrodes.

2. Experimental

2.1. Bacterial Strain and Culture Media

G. sulfurreducens strain PCA (ATCC #51573) was subcultured in our laboratory at 30 °C using a vitamin-free anaerobic medium as described previously [35]. *G. sulfurreducens* was maintained using 100 mM ferrihydrite as an electron acceptor until cells were needed for experiments, at which point cells were transferred into medium containing fumarate (40 mM) as the electron acceptor. After at least 4 transfers using fumarate, cells were used to initiate experiments. Cultures which had been transferred more than 8 times with fumarate as an electron acceptor were discarded.

2.2. Electrode Preparation

Graphite blocks (Toko America, New York NY) were machine-cut into $2 \times 0.5 \times 0.1$ cm electrodes. Freshly cut electrodes were polished using aluminum oxide-silicon carbide sandpaper with grit designation of P400 (3M, Minneapolis MN). Polished electrodes were soaked overnight in 1 N HCl to remove metals and other contaminants, washed twice with acetone and deionized water to remove organic substances, and stored in deionized water. After each experiment, electrode surfaces were cleaned with an additional 1 N NaOH treatment to remove biomass and the entire surface was refreshed through sandpaper polishing and cleaning as described to remove immobilized electron transfer agents.

2.3. Electrode Cell Assembly

Platinum wires from the working electrode were inserted into heat-pulled 3 mm glass capillary tubes (Kimble, Vineland NJ) and soldered inside the capillary to copper wires. Counter electrodes consisted of a 0.1 mm diameter Pt wire (Sigma-Aldrich, St. Louis MO) that was also inserted into a 3 mm glass capillary and soldered to a copper wire. The resistance of each electrode assembly was measured and electrodes with a total resistance higher than 0.5 Ω were discarded. Reference electrodes were connected to bioreactors via a salt bridge assembled from a 3 mm glass capillary and a 3 mm vycor frit (Bioanalytical Systems, West Lafayette IN). Electrode capillaries were inserted through ports in a custom-made Teflon lid that was sealed with a O-ring gasket. This lid fit onto a 20 mL conical electrochemical cell (Bioanalytical Systems, West Lafayette IN), which had been previously soaked in 3 N HNO_3.

After the addition of a magnetic stir bar, the cell was autoclaved and allowed to cool. Following autoclaving, the salt bridge was filled with 0.1 M Na_2SO_4 in 1% agar. A saturated calomel reference electrode (Fisher Scientific, Pittsburgh PA) was placed at the top of this agar layer, and covered in additional Na_2SO_4 to ensure electrical contact. All electrochemical cells were operated under a constant flow of sterile humidified N_2:CO_2 (80:20 v/v), which had been passed over a heated copper column to remove trace oxygen. The electrochemical cells were maintained at 30 °C in a circulating water bath, and mixed via an external magnetic stirrer. Each independent magnetic stirring unit was activated during long-term chronoamperometry (CA) experiments and inactivated during short-term cyclic vol-

tammetry (CV), differential pulse voltammetry (DPV), and square wave voltammetry (SWV).

Autoclaved electrochemical cells, flushed free of oxygen, filled with sterile growth medium, and incubated at 30° were analyzed before each experiment, to verify anaerobicity and the absence of redox active species. Electrochemical cells showing residual peaks in DPV or CV, or baseline noise were discarded as having possible electrode cleanliness or connection noise issues. These verified electrochemical cells were then used for growth of *G. sulfurreducens* cultures.

2.4. Electrochemical Instrumentation

A 16-channel potentiostat (VMP, Bio-Logic USA, Knoxville TN) was connected to the electrochemical cells. Software from the same producer (EC-Lab, V.9.45) was used for data acquisition. CVs at scan rates higher than 100 mV/s were performed using a Gamry PCI4 Femtostat (Gamry Instruments, Warminster PA). Post-acquisition analysis of CV data, such as first derivative and baseline subtraction of CV was performed with the software Utilities for Data Analysis (UTILS), kindly provided by Dr. D. Heering (version 1.0; University of Delft, The Netherlands). All measurements, with exception of CA, were performed in succession without stirring enabled. The parameters for each method were: SWV: $E_i = -0.558$ V vs. SHE $E_f =$ 0.242 V vs. SHE; pulse height 50 mV, frequency 1 Hz, current average over the whole step (1 s, 10 points), accumulation time 5 s. DPV: $E_i = -0.558$ V vs. SHE, $E_f =$ 0.242 V vs. SHE; pulse height 50 mV, pulse width 300 ms, step height 2 mV, step time 500 ms; scan rate 4 mV/s, current average over the last 80% of the step (1 s, 12 points), accumulation time 5 s. CV: equilibrium time 5 s., scan rate 1 mV/s, $E_i = -0.558$ V vs. SHE, $E_f = 0.242$ V vs. SHE, current averaged over the whole step (1 s, 10 points). CA: $E = 0.242$ V vs. SHE.

2.5. Single Turnover Voltammetry

To remove electron donor, growth medium was exchanged with a medium without acetate, while maintaining anaerobic conditions. Biofilms were then starved until anodic (oxidation) current decreased to less than 1 μA. CV was performed at increasing scan rate, from 1 mV/s to 2 V/s.

2.6. Determination of Attached Biomass

The electrodes were rinsed in sterile growth medium to remove loosely attached cells. Attached proteins were then solublized by heating in a small volume of 0.2 N NaOH and analyzed through bicinchoninic acid (BCA) protein assay kit (Thermo Scientific, Rockford IL).

3. Results and Discussion

3.1. Effect of Inoculum on Colonization and Growth Rates

In all experiments, electrochemical reactors were inoculated with planktonic *G. sulfurreducens* cells within 1 h of entering stationary phase due to exhaustion of electron donor (fumarate). When an oxidizing potential of +0.24 V vs. SHE was applied, a sustained current reflecting catalytic oxidation of acetate by cells and reduction of the electrode was observed (Fig. 1A). As previous work focused on biofilms after they became fully developed [35], the dynamics of early attachment and growth were investigated. Three distinct phases could be detected in all experiments (Fig. 1A). First, within 3–6 h of inoculation, oxidation current increased faster than reported growth rates for *G. sulfurreducens* (typically doubling within 2 h). Second, after this initial rise, but below current densities of ca. 300 μA/cm^2, current increased exponentially with a doubling time of ca. 6 hours, regardless of inoculum size. Finally, above current densities of ca. 300 μA/cm^2, the rate of increase slowed as current production rates approached values as high as 1000 μA/cm^2 (Fig. 1B).

Example data in Figure 1A shows the effect of inoculum size on the early phases of colonization and growth; when a higher cell density was added, the magnitude of the initial increase was larger, consistent with this first phase reflecting attachment by planktonic cells. Replacement of medium after this initial attachment phase (e.g., at 24 h), did not alter subsequent growth rates or current densities, demonstrating that the primary source of new cells was doubling of cells attached to the electrode, not further colonization by planktonic cells. Also, addition of acetate or fresh medium at the point when current increase slowed had no effect, indicating that current stabilization was not due to depletion of electron donors, substrate diffusion into the biofilm, or lack of other nutrients.

Routine use of a 20% inoculum allowed a sustained exponential phase, in which doubling time averaged 5.8 h over nearly a 40 h period. In all of these experiments, the length of the exponential phase was not dependent upon the length of incubation, but rather on biofilms achieving a current density exceeding ca. 300 μA/cm^2.

3.2. Relationship Between Attached Biomass and Current Production

Previous reports have shown that anodic current increased linearly with increasing *G. sulfurreducens* electrode colonization and biofilm thickness [23]. This observation implies that each cell in the biofilm is respiring at a similar rate, from the first cells to make contact, to cells located at increasing distances from the surface. However, the phases observed in this study at specific current densities suggested that bacteria in the biofilms experienced changing conditions. To examine this relationship, independent electrodes were

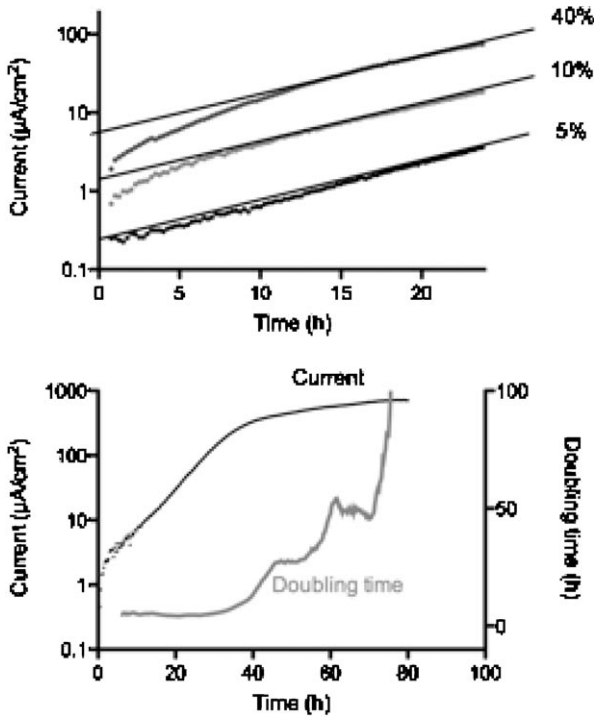

Fig. 1. (A) Chronoamperometry showing relationship between inoculum level and initial current production rate. (B) Chronoamperometry over a complete growth experiment for a 20% inoculum, showing the fast doubling time while current density is below 300 μA/cm^2, and progressive slowing afterwards.

inoculated and harvested at different levels of colonization, and protein attached to electrodes was measured.

To determine when biofilms were transitioning beyond the monolayer stage, levels of attached protein were correlated with confocal microscopy images of identical electrodes, (representative images are available in two previous works, [35, 36], and are also similar to [23]). According to these measurements, monolayer coverage of *G. sulfurreducens* occurred near levels of attached protein of ca. 20 μg/cm^2, (or current densities of <75 μA/cm^2). These values can be compared to estimates based on standard protein:cell ratios (0.3×10^{-6} μg protein:cell [37], and an assumption that a cell occupies ca. 1 μm^2); which produces a similar monolayer estimate at 30 μg/cm^2. As cells reached the end of the first exponential stage (ca. 300 μA/cm^2), the biofilm thickness was clearly on the order of 10 μm, representing multicellular biofilms. Final biofilms (>750 μA/cm^2) exceeded 20 μm, similar to previous observations [23, 35, 36].

Therefore, the data shown in Figure 2 is equivalent to a series of electrodes harvested within the first hours of inoculation (e.g. at current densities <25 μA/cm^2, before electrodes were completely covered in cells), through exponential phase (50–300 μA/cm^2, as cells grew in multiple layers), until nearly 96 h after inoculation (<750 μA/cm^2), as biofilm growth slowed, and reached 20 μm thickness.

One of the most striking results of this series was that at very early time points, the first biomass to attach supported a much lower rate of electron transfer (per unit of protein) than at later time points. In other words, the very first cells attached to electrode surfaces demonstrated a respiration rate as low as 2–4 μA/μg protein. However, this ratio quickly increased to a stable rate of nearly 8 μA/μg protein, reaching its maximum value in the same window (100–300 μA/cm^2) that supported maximum growth rates. These observations revealed a significant increase in the specific rate of electron transfer was taking place during the first hours of colonization.

When maximum ratios of current production (8 μA/μg) were expressed as a specific rate of respiration (1 A = 96,485 mol e$^-$/s), a value of 0.3 mmol electrons/mg protein/h was obtained. This rate of respiration was very similar to values obtained for *G. sulfurreducens* in chemostats with Fe(III)-citrate as the electron acceptor (0.28 mmol electrons/mg protein/h, assuming biomass is 50% protein) [38]. This demonstrated that *Geobacter* can respire to solid surfaces as fast as it can respire to soluble compounds, provided the surface remains at a favorable consistent potential with available sites for future growth.

These measurements also allowed estimates of growth yield on electrodes for exponentially growing *G. sulfurreducens*. As biomass primarily came from planktonic cells during the initial colonization phase, data was only taken from exponentially growing (100–300 μA/cm^2) electrodes.

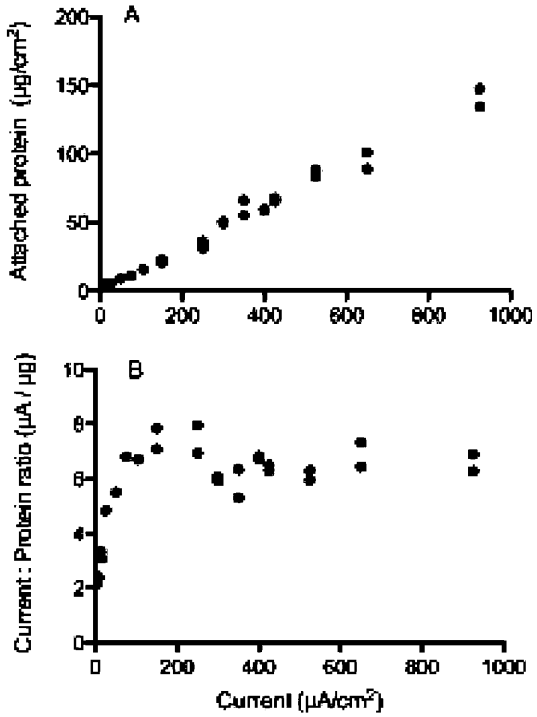

Fig. 2. (A) Relationship between current density and attached protein, expressed per unit geometric surface area. (B) Ratio between attached protein and current density, showing low specific rates of respiration during the first stages of colonization. Cells grown to stationary phase using fumarate, a soluble electron acceptor, were used to initiate experiments.

The charge (Q) transferred to the electrode (expressed in Coulombs) relative to the increase in biomass yielded an average value of 342 mg protein/mol electrons ($n = 6$). For comparison, chemostat and modeling yield estimates for *G. sulfurreducens* grown with Fe(III)-citrate on the order of 300 mg protein/mol e^- have been reported [38, 39], suggesting that electron transport (ATP/e^-) and biomass accumulation with soluble metals has similar efficiency as growth with acceptors such as electrodes.

3.3. Effect of Stage of Growth on Voltammetry of Biofilms

Representative voltammetry analyses of *G. sulfurreducens* biofilms at different key growth stages are shown in Figure 3. The electrochemical parameters of growing biofilms were measured in at least 10 independent biological replicates, and variance between replicates was typically less than 5% [35]. The primary finding of these trials was the consistency of the sigmoidal catalytic wave, with an onset potential near -0.2 V vs. SHE, and a maximum limiting current near -0.05 V. A small reversible peak at -0.08 V vs. SHE could also be resolved in all biofilms. At early time points, first derivative analysis of CV data (Fig. 4B) showed a symmetrical maximum (near -150 mV), which broadened and shifted slightly more negative as biofilms grew [26]. Replacement of the medium, which removed planktonic cells and possible electron shuttles, had no effect on voltammetry results (e.g., second trace in Fig. 4A). As we recently observed some redox shuttles can be retained by biofilms or electrodes [21], some biofilms were subjected to multiple medium changes (as many as 5), followed by voltammetry, with no measured effect.

3.4. Effect of Short-Term Growth at Lower Potential

Voltammetry data shown in Figure 3 supported a model in which the dominant mechanism and rate-controlling steps in electron transport were not significantly changing during growth of biofilms at $+0.24$ V. However, in the environment, in microbial fuel cells, and perhaps at the outer edges of biofilms, cells may experience variability, or less favorable driving forces for electron transfer. To investigate the

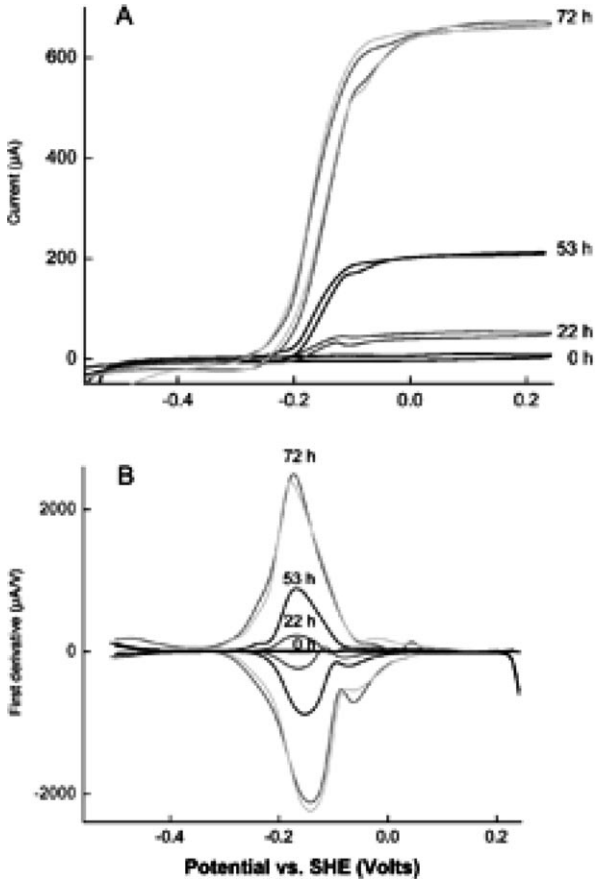

Fig. 3. (A) Representative cyclic voltammetry (1 mV/s) of biofilms at different stages of growth at $+0.24$ V vs. SHE (22, 53, and 72 h). At 72 h, medium was removed and replaced with fresh medium, and voltammetry was repeated (overlying trace). (B) First derivative plots of CV data, showing midpoint potentials of catalytic waves and additional features in CV.

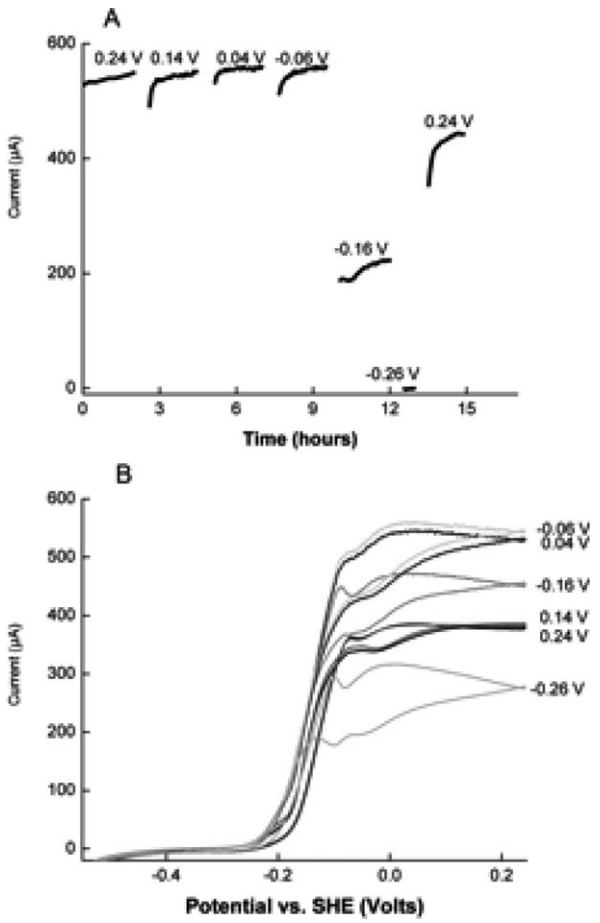

Fig. 4. (A) Representative chronoamperometry of biofilms subjected to progressively lower potentials (3 h each). (B) In between each potential step, cyclic voltammetry (1 mV/s) was performed, producing a 'discharge' during the anodic sweep.

response of cells to lower potential, biofilms grown to plateau phase at +0.24 V vs. SHE were poised at lower electrode potentials, and held for 3 h at each potential. In between each step, voltammetry analyses were performed. The purpose of this sequence was to keep biomass and electron transfer capacity on the electrode relatively constant, while testing the effect of electron acceptor limitation.

Amperometry of a representative experiment (repeated with 4 independent electrodes) is shown in Figure 4A. Sustained anodic current did not change appreciably, even when electrode potential was lowered by nearly 0.2 V (to −0.06 V), an observation consistent with cyclic voltammetry data. Also consistent was the severe effect of a drop to potentials lower than −0.1 V At a potential of −0.26 V, bacteria were unable to transfer electrons to the electrode. If held at the lowest potential (−0.26 V) for 3 hours, biofilms required 3–6 h to recover original rates of electron transfer when returned to +0.24 V, indicating possible down-regulation of capacity, or damage to biofilms.

When cells were held at +0.04 V and −0.06 V, even though their steady state anodic (oxidation) currents were similar (Fig. 4A), CV showed an increase in limiting current, especially during the oxidation (anodic) scan (Fig. 4B). The fact that this current increase was not sustained in the reverse scan was consistent with electrons accumulating in proteins with a potential of about 0 V vs. SHE, and discharging upon the application of higher potential during the CV. When held at even lower potentials (−0.16 and −0.26 V), biofilms still demonstrated the 'discharge' effect in anodic current when scanned via CV, with the midpoint of the catalytic wave shifting toward more negative values, as could be expected when substrate oxidation rate is in excess relative to the charge-carrying process [40, 41]. No new redox-active species were detected during these experiments, although exposure to −0.26 V significantly reduced the response of cells, consistent with the fact that biofilms did not recover to normal electron transfer rates when returned to the original oxidizing potential of +0.24 V.

3.5. Effect of Growth at Lower Potential

To test if *G. sulfurreducens* could significantly alter their external electron transfer pathway when subjected to growth at lower potentials, biofilms were grown from inoculation at −0.16 V vs. SHE. At this potential, slow growth (with a generation time of over 12 h), was supported for a period of over 6 days. These biofilms were also subjected to voltammetry over time, and Figure 5 shows representative results ($n = 4$).

G. sulfurreducens grown at lower potentials still produced sigmoidal catalytic waves with similar onset and midpoint potentials as biofilms grown at higher potentials to similar current density (Fig 5B). In addition, reversible peaks near the top of the catalytic wave, well above the poised potential of the electrode, were still present. Long-term growth at this lower potential did not produce the 'charge accumulation' effect in cyclic voltammetry observed with cultures grown at higher potentials.

To more accurately compare the electrochemistry of biofilms grown at these two potentials, biofilms were grown at both high potential (+0.24 V) or low potential (−0.16 V), until each biofilm was producing the same sustained current. Figure 6 shows cyclic voltammetry from representative high- and low-potential biofilms at similar stages of anodic current production. The similar onset, steepness, and secondary features of the two biofilms could be more clearly seen using this comparison.

In past studies, we have used pulse techniques to detect redox species within actively respiring biofilms. Because a central question of this high vs. low potential growth experiment was whether these conditions elicited a change in redox proteins catalyzing electron transfer, respiring biofilms were also analyzed through differential pulse voltammetry (DPV) and square wave voltammetry (SWV) over a range of frequencies, to increase peak resolution within these biofilms. Representative DPV data indicated the presence of at least two alterations when grown at −0.16 V, compared to growth at higher potentials (+0.24 data).

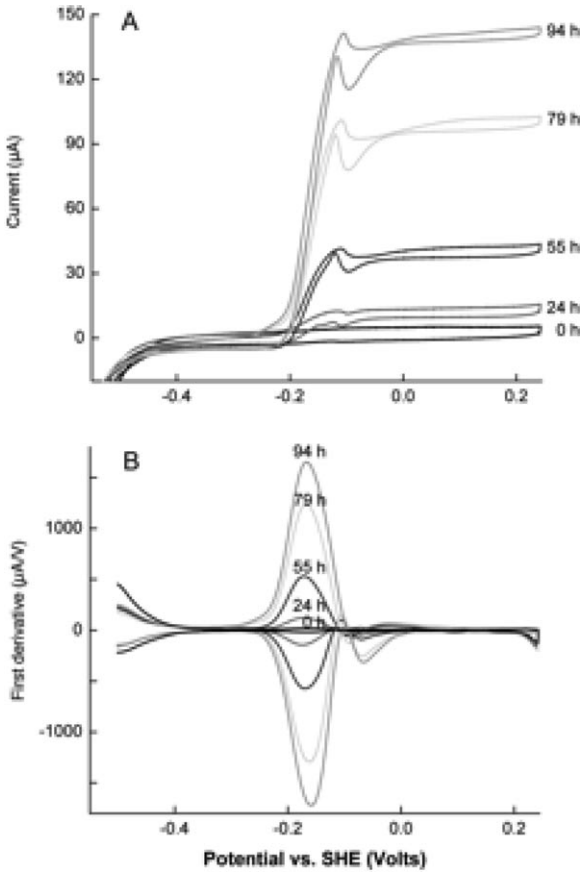

Fig. 5. (A) Representative cyclic voltammetry (1 mV/s) of biofilms at different stages of growth at −0.16 V vs. SHE (24, 55, and 79 and 94 h). (B) First derivative plots of CV data, showing midpoint potentials of catalytic waves and additional features in CV.

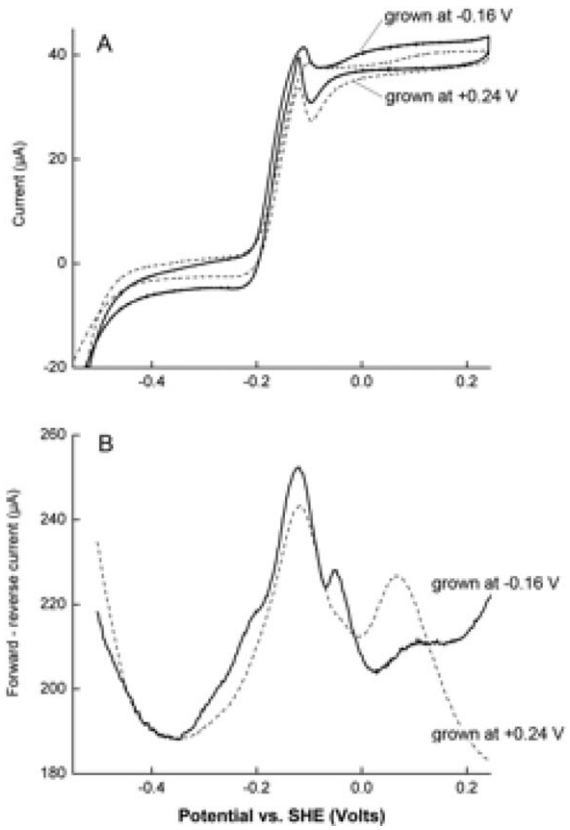

Fig. 6. For more accurate comparison between biofilms grown at $+0.24$ V and -0.16 V vs. SHE, biofilms were grown to identical current densities and subjected to (A) CV (1 mV/s), and (B) Differential pulse voltammetry (see methods for parameters).

Further attempts to resolve these differences using higher frequency pulse methods, such as square wave voltammetry (SWV) were attempted. No additional peaks were detected or separated by SWV, and most features were not detected at frequencies above 10 Hz, suggesting that peaks observed in biofilms corresponded to relatively slow electron transfer processes. We note that SWV at variable frequencies and with higher pulse heights damaged biofilms (as measured by recovery of biofilms after return to poised-potential conditions). Thus, while pulse techniques such as DPV and SWV can be valuable in the study of purified proteins [42], and holds promise at estimating interfacial electron transfer rates, it should be used with caution when analyzing viable biofilms.

3.6. Single-Turnover Cyclic Voltammetry

When cells are oxidizing substrates, the catalytic current recorded during a voltammetry sweep represents multiple turnovers of each redox species, and the high catalytic current may obscure signals from individual redox species. By analyzing biofilms under nonturnover conditions, properties related to interfacial electron transfer between multiple redox species, or between redox centers, can be studied. These rates and phenomena are not dependent on such factors as diffusion of compounds into the biofilm, or the respiration rate of bacteria.

To first verify that the approach of removing donors did not significantly alter the physiology of biofilms, a series of starvation experiments were conducted. Starvation of fully grown *G. sulfurreducens* biofilms to eliminate catalytic features (e.g. to reduce the height of the catalytic wave from >750 μA/cm^2 to <2 μA/cm^2) required at least 24 hours, suggesting the presence of internal storage compounds. After this starvation procedure, addition of acetate immediately restored 50–60% of the original maximal current, and biofilms typically returned to original levels within 12 h. Importantly, CV and DPV analysis of these biofilms before and after the starvation procedure produced identical results to those shown in Fig. 3, demonstrating that the electron transfer mechanism of the previously starved cells was unchanged. In addition, starvation for 24 hours produced results (in terms of peak heights, electrode coverage estimates, and scan rate analysis results) that were within 10% of the same biofilms starved for over 48 h, indicating that significant detachment, degradation, or down-regulation, did not occur beyond this point.

A typical result, with and without baseline subtraction, is shown in Figure 7. Of particular interest was a redox couple centered at -0.108 ± 0.002 V vs. SHE (A in Fig. 7), as well as a second redox couple (B in Fig. 7) at -0.056 ± 0.004 V, and a poorly reversible reduction peak (C in Fig. 7) at -0.235 ± 0.003 V vs. SHE (all midpoint potentials from $n = 6$ independent biofilms). Several small features were present, but were too small or close to major peaks to accurately determine their potential. The apparent number of electrons transfer for each peak was not estimated (based on peak width), because of partial overlapping of peaks.

Thin-film behavior could not be observed (linear dependence of peak height on scan rate), demonstrating that as scan rate was increased from these relatively slow scan rates (1 mV/s), less of the film was being discharged. The number of redox species accessible to the electrode at 1 mV/s, estimated through the peak current [43] was 1.66 ± 0.45, 2.56 ± 0.61, and 0.62 ± 0.04 nmol/cm^2 for species A, B, C, respectively. At all scan rates, peak heights were proportional to the square root of scan rate, indicating a diffusional limitation preventing electrons in the film from reaching the electrodes at faster time scales. This behavior was consistent with the interfacial reaction (the final hop of electrons from redox proteins to the electrode) always being more rapid than reactions responsible for bringing electrons through the biofilm to this interface.

3.7. Characteristics of the Cell–Electrode Interface

This data summarizes over 100 independent biological experiments where *G. sulfurreducens* was grown using electrodes as electron acceptors. By reducing the variability of electrode surfaces through polishing and cleaning, utilizing defined inocula (grown to the same point of electron acceptor depletion), and focusing on unique stages of

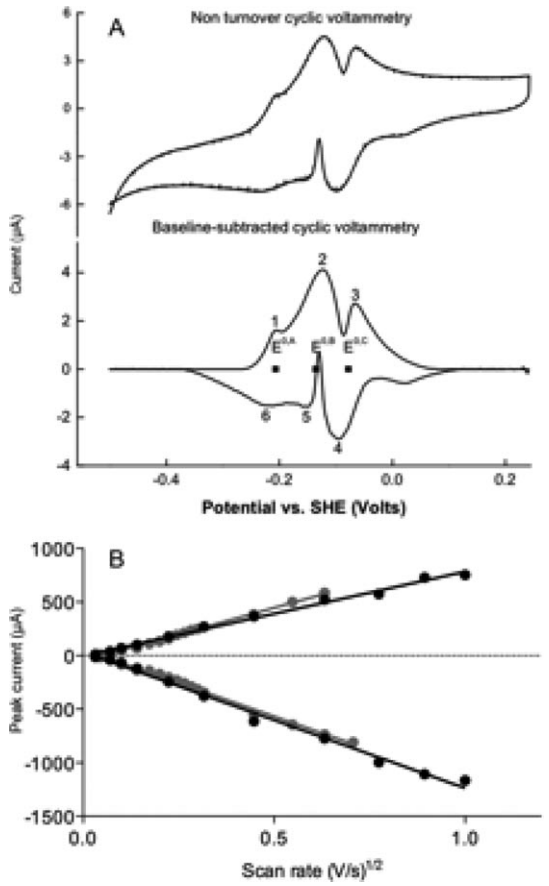

Fig. 7. (A) Representative cyclic voltammetry (1 mV/s) of biofilm starved of electron donors for 24 h, showing baseline-subtracted data. (B) Comparison of baseline-subtracted peak heights for two independent films subjected to increasing scan rates, showing linear dependence on the square root of scan rate.

biofilm development, we were able to quantify apparent growth rates, yield, and electron transfer rates by this model metal-reducing bacterium at different growth stages and across a range of thermodynamic conditions. In general, these experiments reveal an early phase where this pathway must be established, and a subsequent network of redox proteins connecting cells to surfaces that is remarkably consistent, and able to communicate electrons across relatively long distances, with little change in the overall mechanism.

G. sulfurreducens shows rapid self-assembly on electrodes, and even cells grown with soluble fumarate as an electron acceptor are apparently immediately capable of some degree of extracellular electron transfer. For an organism selected in the environment (and the laboratory) for interactions with charged Fe(III) and Mn(IV) surfaces, the increase in anodic (oxidation) current reflects a fortuitous affinity between cells and polycrystalline graphitic electrodes, as well as favorable orientation of at least one redox protein close enough to the surface to allow direct electron transfer. However, the low electron transfer rates per unit of initially attached protein (Fig. 2) also shows that these first colonizers may not possess a full complement of redox proteins, or their redox proteins are not yet in optimal contact with electrodes, analogous to how many bacteria require retraction of type IV pili or flagellar motility to overcome local electrostatic interactions and firmly adhere to surfaces.

The fact that rates of growth following this initial attachment phase rivaled those of planktonic cells utilizing soluble Fe(III) showed that electron transfer across this cell-electrode connection was not limiting, in terms of its ability to carry electrons from cells to the electrode surface. This rate could be sustained for days when the lowest levels of inoculum were used, (Fig 1B), and was never affected by removal of planktonic bacteria. Individual *G. sulfurreducens* cells can clearly respire, generate ATP, and double as fast using an insoluble acceptor (in this case an electrode) as with a soluble acceptor, when the surface area and attachment is not a limiting factor.

While the first layers of cells experience near-optimal conditions, the slowing rate of anodic current increase as colonization progressed revealed a developing limitation to electron transfer as multiple cell layers were added. A simple hypothesis for this could be the transition from daughter cells being able to expand in two (sideways or upwards), to only one (upwards) dimension, limiting the area available for new colonization. The final plateau in current density suggests the existence of a barrier to accumulation of a biofilm beyond this thickness. Multiple researchers have proposed 'proton escape' from the thickening biofilm as a key factor in this limit [44–46]. This calculation explains forces that oppose charge transfer, and agrees well with many experimental observations. It does not explain why these high rates of respiration (e.g., the high current/unit protein) are not resulting in progressively thicker biofilms. To explain this phenomenon, cells may be responding to the lack of available expansion (within the biofilm) or attachment (on top of the biofilm) sites, or may be expending significant metabolic energy to compensate for local pH differences.

We observed no evidence for a dramatic change in the redox interface, or model for electron transfer between cells and electrodes at any phase of growth. At all time points, the rate-controlling electron transfer process was centered at a similar potential, and resistive behavior or new electron transfer reactions were not detected. No unusual waveforms appeared at later stages of growth, which would have suggested developing heterogeneity in protein orientation or binding. This has significant implications for simplifying the model of electron transfer from cells to electrodes, as was described by [26].

3.8. Insights from Lower Potential Experiments

Another surprising finding was that, even when grown at +0.24 V, *G. sulfurreducens* reached its maximum rate of electron transfer at a driving force of about −0.05 V, essentially ignoring over 50% of the energy in the available electron acceptor. Even when grown at lower potential

(−0.16 V), use of the same electron transfer scheme caused *G. sulfurreducens* to operate at about half maximal velocity (as shown by the increased respiration rate of cells when the potential was raised during a CV). Thus, *G. sulfurreducens* showed little short-term ability to 'tune' its outer membrane interface to take advantage of available energy, and showed only slightly altered higher potential redox proteins detectable at the surface in response to lower potentials (Fig. 6). While *Geobacter* has an unprecedented number of outer membrane cytochromes in its genome, and has shown genomic plasticity in its ability to evolve in response to mutations or selective pressure [47], this redox protein diversity does not appear to be significantly altered in response to external potential without significant evolutionary pressure.

Biofilms exposed to moderately lower potentials for a few hours (such as −0.05 V), did not slow their overall rate of electron transfer, exactly what would be predicted from slow scan rate CV analysis. However, upon raising the potential during a subsequent CV, a discharge across a broad potential range was observed (Fig. 4B), consistent with a pool of higher potential proteins in or on the cell, or distributed between cells. This caching of electrons in redox proteins is consistent with Lovley's hypothesis for excess hemes as sites for 'storage', proposed recently [48]. Such a large pool of membrane-attached, or interstitial redox proteins, is also reminiscent of redox polymers, designed to relay electrons from enzymes to surfaces [49].

3.9. Single-Turnover Voltammetry

G. sullfurreducens biofilms remained intact and did not alter their pattern of detectable redox-active species, even after 24 h of starvation. This allowed detection of a complex pattern of redox-active species that was greatly in excess (nmol/cm^2) of protein monolayers formed on electrodes (pmol/cm^2), even when the multiheme nature of *Geobacter* cytochromes was taken into account. This provided further evidence for the long-range communication of a large array of redox proteins between the surface and cells.

The relationship between scan rate and peak height measured in *G. sulfurreducens* single-turnover voltammetry was indicative of semi-infinite diffusion behavior. In other words, the biofilms did not discharge as a single film, but fewer electrons reached the electrode as the experiment timescale was reduced, and the dependence on the square root of scan rate suggests a diffusional (Fick's Law) limitation to electron movement. Since the apparent diffusion coefficient is primarily a function of redox center concentration biofilm thickness, further work using accurate biofilm volume measurements and heme concentrations may be able to provide estimates of this important constraint on electron transfer.

Acknowledgements

We thank the Initiative for Renewable Energy and Environment (IREE) and the NSF (Grant DBI-0454861) for their support. Jian Sun was supported by a joint research Fellowship from the South China University of Technology.

References

[1] D. R. Lovley, *Geobiology* **2008**, *6*, 225.
[2] D. R. Lovley, *Curr. Opin. Biotechnol.* **2008**, *19*, 564.
[3] J. A. Gralnick, D. K. Newman, *Mol. Microbiol.* **2007**, *65*, 1–11.
[4] K. T. Finneran, C. V. Johnsen, D. R. Lovley, *Int. J. Syst. Evol. Microbiol.* **2003**, *53*, 669.
[5] J. D. Coates, D. J. Ellis, C. V. Gaw, D. R. Lovley, *Int. J. Syst. Bacteriol.* **1999**, *49*, 1615.
[6] L. Shi, T. C. Squier, J. M. Zachara, J. K. Fredrickson, *Mol. Microbiol.* **2007**, *65*, 12.
[7] D. R. Lovley, in *Environmental Microbe-Metal Interactions* (Ed: D. R. Lovley), ASM Press, Washington, D.C. **2000**; pp. 3–30.
[8] D. R. Lovley, in *The Prokaryotes: An Evolving Electronic Resource for the Microbiological Community,* 3rd ed. (Eds: M. Dworkin, S. Falkow, E. Rosenberg, K.-H. Schleifer, E. Stackebrandt), Springer, Heidelberg **2000**.
[9] J. R. Lloyd, D. R. Lovley, *Curr. Opin. Biotechnol.* **2001**, *12*, 248.
[10] R. T. Anderson, H. A. Vrionis, I. Ortiz-Bernad, C. T. Resch, P. E. Long, R. Dayvault, K. Karp, S. Marutzky, D. R. Metzler, A. Peacock, D. C. White, M. Lowe, D. R. Lovley, *Appl. Environ. Microbiol.* **2003**, *69*, 5884.
[11] K. T. Finneran, R. T. Anderson, K. P. Nevin, D. R. Lovley, *Soil Sediment Contam.* **2002,** *11*, 339.
[12] A. K. Lee, D. K. Newman, *Appl. Microbiol. Biotechnol.* **2003,** *62*, 134.
[13] W. A. Hamilton, *Biofouling* **2003**, *19*, 65.
[14] J. Biffinger, M. Ribbens, B. Ringeisen, J. Pietron, S. Finkel, K. Nealson, *Biotechnol. Bioeng.* **2008**, *102*, 436.
[15] M. Lanthier, K. B. Gregory, D. R. Lovley, *FEMS Microbiol. Lett.* **2008**, *278*, 29.
[16] D. R. Lovley, *Nature Rev. Microbiol.* **2006**, *4*, 497.
[17] Y. Zuo, D. F. Xing, J. M. Regan, B. E. Logan, *Appl. Environ. Microbiol.* **2008,** *74*, 3130.
[18] L. Ieropoulos, J. Greenman, C. Melhuish, J. Hart, *J. Power Sources* **2005**, *145*, 253.
[19] D. Coursolle, D. B. Baron, D. R. Bond, J. A. Gralnick, *J. Bacteriol.* **2009**, *192*, 467.
[20] H. von Canstein, J. Ogawa, S. Shimizu, J. R. Lloyd, *Appl. Environ. Microbiol.* **2008**, *74*, 615.
[21] E. Marsili, D. B. Baron, I. D. Shikhare, D. Coursolle, J. A. Gralnick, D. R. Bond, *Proc. Natl. Acad. Sci. USA* **2008**, *105*, 3968.
[22] G. Reguera, R. B. Pollina, J. S. Nicoll, D. R. Lovley, *J. Bacteriol.* **2007**, *189*, 2125.
[23] G. Reguera, K. P. Nevin, J. S. Nicoll, S. F. Covalla, T. L. Woodard, D. R. Lovley, *Appl. Environ. Microbiol.* **2006**, *72*, 7345.
[24] G. Reguera, K. D. McCarthy, T. Mehta, J. S. Nicoll, M. T. Tuominen, D. R. Lovley, *Nature* **2005**, *435*, 1098.
[25] X. Qian, G. Reguera, T. Mester, D. R. Lovley, *FEMS Microbiol. Lett.* **2007**, *277*, 21.
[26] H. Richter, K. P. Nevin, H. F. Jia, D. A. Lowy, D. R. Lovley, L. M. Tender, *Energy Environ. Sci.* **2009**, *2*, 506.

[27] J. R. Lloyd, C. Leang, A. L. Hodges Myerson, M. V. Coppi, S. Cuifo, B. Methe, S. J. Sandler, D. R. Lovley, *Biochem. J.* **2002**, *369*, 153.
[28] T. Mehta, M. V. Coppi, S. E. Childers, D. R. Lovley, *Appl. Environ. Microbiol.* **2005**, *71*, 8634.
[29] B. C. Kim, B. L. Postier, R. J. DiDonato, S. K. Chaudhuri, K. P. Nevin, D. R. Lovley, *Bioelectrochemistry* **2008**, *73*, 70.
[30] T. Mehta, S. E. Childers, R. Glaven, D. R. Lovley, T. Mester, *Microbiology* **2006**, *152*, 2257.
[31] B. C. Kim, C. Leang, Y. H. Ding, R. H. Glaven, M. V. Coppi, D. R. Lovley, *J. Bacteriol.* **2005**, *187*, 4505.
[32] B. C. Kim, D. R. Lovley, *FEMS Microbiol. Lett.* **2008**, *286*, 39.
[33] K. Juarez, B. C. Kim, K. Nevin, L. Olvera, G. Reguera, D. R. Lovley, B. A. Methe, *J. Mol. Microbiol. Biotechnol.* **2009**, *16*, 146.
[34] S. Srikanth, E. Marsili, M. C. Flickinger, D. R. Bond, *Biotechnol. Bioeng.* **2008**, *99*, 1065.
[35] E. Marsili, J. B. Rollefson, D. B. Baron, R. M. Hozalski, D. R. Bond, *Appl. Environ. Microbiol.* **2008**, *74*, 7329.
[36] J. B. Rollefson, C. E. Levar, D. R. Bond, *J. Bacteriol.* **2009**, *191*, 4207.
[37] P. P. Dennis, H. Bremer, *J. Bacteriol.* **1974**, *119*, 270.
[38] A. Esteve-Nunez, M. Rothermich, M. Sharma, D. Lovley, *Environ. Microbiol.* **2005**, *7*, 641.
[39] R. Mahadevan, D. R. Bond, J. E. Butler, A. Esteve-Nunez, M. V. Coppi, B. O. Palsson, C. H. Schilling, D. R. Lovley, *Appl. Environ. Microbiol.* **2006**, *72*, 1558.
[40] J. Hirst, *Biochim. Biophys. Acta* **2006**, *1757*, 225.
[41] J. N. Butt, J. Thornton, D. J. Richardson, P. S. Dobbin, *Biophys. J.* **2000**, *78*, 1001.
[42] L. J. Jeuken, A. K. Jones, S. K. Chapman, G. Cecchini, F. A. Armstrong, *J. Am. Chem. Soc.* **2002**, *124*, 5702.
[43] A. J. Bard, L. R. Faulkner, *Electrochemical Methods*, 2nd ed., Wiley, Chichester **2001**.
[44] C. I. Torres, A. Kato Marcus, B. E. Rittmann, *Biotechnol. Bioeng.* **2008**, *100*, 872.
[45] C. I. Torres, H. Lee, B. E. Rittmann, *Environ. Sci. Technol.* **2008**, *42*, 8773.
[46] A. E. Franks, K. P. Nevin, H. F. Jia, M. Izallalen, T. L. Woodard, D. R. Lovley, *Energy Environ. Sci.* **2009**, *2*, 113.
[47] H. Yi, K. P. Nevin, B. C. Kim, A. E. Franks, A. Klimes, L. M. Tender, D. R. Lovley, *Biosens. Bioelectron.* **2009**, *24*, 3498.
[48] A. Esteve-Nunez, J. Sosnik, P. Visconti, D. R. Lovley, *Environ. Microbiol.* **2008**, *10*, 497.
[49] A. Heller, *Curr. Opin. Chem. Biol.* **2006**, *10*, 664.

